optica

Compact intense extreme-ultraviolet source

B. Major,[1,2,5,†] O. Ghafur,[3,†] K. Kovács,[4] K. Varjú,[1,2] V. Tosa,[4] M. J. J. Vrakking,[3] and B. Schütte[3,6]

[1]ELI-ALPS, ELI-HU Non-Profit Ltd., Wolfgang Sandner utca 3., Szeged 6728, Hungary
[2]Department of Optics and Quantum Electronics, University of Szeged, Dóm tér 9, Szeged 6720, Hungary
[3]Max-Born-Institut, Max-Born-Strasse 2A, 12489 Berlin, Germany
[4]National Institute for Research and Development of Isotopic and Molecular Technologies, Donat str. 67-103, 400293 Cluj-Napoca, Romania
[5]e-mail: Balazs.Major@eli-alps.hu
[6]e-mail: Bernd.Schuette@mbi-berlin.de

Received 3 February 2021; revised 29 April 2021; accepted 29 May 2021 (Doc. ID 421564); published 25 June 2021

High-intensity laser pulses covering the ultraviolet to terahertz spectral regions are nowadays routinely generated in a large number of laboratories. In contrast, intense extreme-ultraviolet (XUV) pulses have only been demonstrated using a small number of sources including free-electron laser facilities and long high-harmonic generation (HHG) beamlines. Here, we demonstrate a concept for a compact intense XUV source based on HHG that is focused to an intensity of 2×10^{14} W/cm^2, with a potential increase up to 10^{17} W/cm^2 in the future. Our approach uses tight focusing of the near-infrared (NIR) driving laser and minimizes the XUV virtual source size by generating harmonics several Rayleigh lengths away from the NIR focus. Accordingly, the XUV pulses can be refocused to a small beam waist radius of 600 nm, enabling the absorption of up to four XUV photons by a single Ar atom in a setup that fits on a modest (2 m) laser table. Our concept represents a straightforward approach for the generation of intense XUV pulses in many laboratories, providing exciting opportunities for XUV strong-field and nonlinear optics experiments, for XUV-pump XUV-probe spectroscopy and for the coherent diffractive imaging of nanoscale structures.

https://doi.org/10.1364/OPTICA.421564

1. INTRODUCTION

Nonlinear optical techniques have widespread applications including frequency mixing [1–3], Raman amplification [4], Kerr-lens modelocking [5], and self-phase modulation [6,7]. In the long-wavelength range, the development of compact and efficient secondary terahertz sources with microjoule energies [8] has boosted the field of nonlinear terahertz optics [9]. The situation is different in the extreme ultraviolet (XUV) and x-ray wavelength range, where the generation of high pulse energies in combination with high intensities has only been demonstrated at a limited number of facilities including free-electron lasers (FELs) [10–12] and long (≥10 m) high-harmonic generation (HHG) beamlines [13–18]. While first nonlinear XUV optics experiments including multiphoton absorption [19–21], four-wave mixing [22], and XUV-XUV pump–probe spectroscopy [23] have been performed, the large size and complexity of existing experimental setups using intense XUV pulses impede faster progress in this field, which would benefit from more compact and less complex setups. Such sources would, furthermore, pave the way to the application of powerful techniques like attosecond-pump attosecond-probe spectroscopy [15,24] and coherent diffractive imaging of nanoscale structures and nanoparticles [14,25,26] in a much larger number of laboratories than is currently the case.

Our concept for a compact intense XUV source is based on HHG, which has traditionally been performed at or close to the focal plane of the fundamental laser [3] because of the high driving light intensities ($\approx 10^{14}$W/cm^2) that are required for efficient HHG. After more powerful driving lasers became available, loose-focusing geometries were adopted [13–18], in which the fundamental laser is focused by a lens or a spherical mirror with a long focal length on the order of 10 m. This increases the focus size of the fundamental laser, leading to a large volume from which high harmonics are emitted and resulting in XUV pulses with microjoule energies [13,20,27]. A crucial disadvantage of this approach is its complexity and its intrinsic requirement of a large laboratory. Moreover, this approach does not readily lead to higher XUV intensities, since the XUV source size grows proportionally to the focal length that is used [28], and source demagnification factors that can be achieved using focusing optics are finite.

Previous studies showed that placing the HHG medium away from the driving laser focal plane can be used to optimize the macroscopic generation conditions [29–31] and can result in optics-less focusing of the XUV beam [32]. Here, we aim at increasing the focused XUV intensity in a compact setup and propose to generate high harmonics several Rayleigh lengths away from the focal plane of the driving laser, employing a focusing element with a relatively short focal length of 1 m [see Fig. 1(a)]. As schematically shown in Fig. 1(b), this leads to a situation where the driving laser wavefronts in the HHG medium are curved, resulting in curved wavefronts of the generated XUV pulses [33]. Due to the short

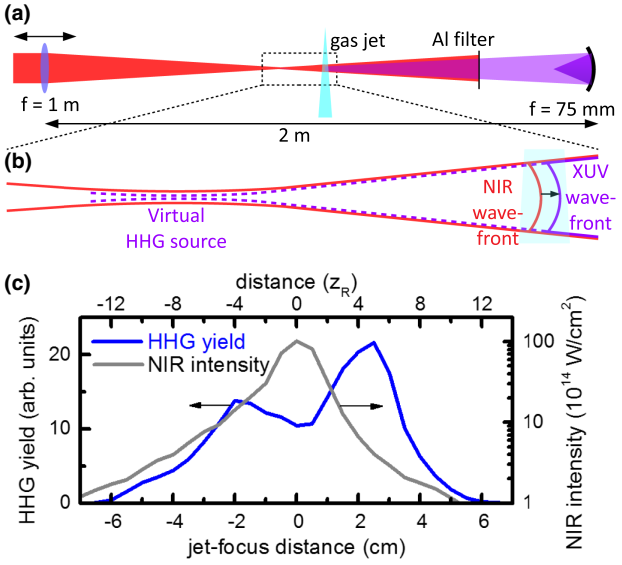

Fig. 1. Compact intense XUV source. (a) Experimental setup: NIR driving pulses with a duration of 40 fs and a pulse energy of up to 16 mJ are focused using a spherical lens with $f = 1$ m. HHG takes place in a high-pressure gas jet that is placed in the converging or diverging NIR beam. An Al filter attenuates the NIR pulses after HHG, and the XUV pulses are focused to high intensities by a spherical mirror with $f = 75$ mm. (b) Zoom into the generation region, visualizing the transfer of curved wavefronts from the fundamental to the harmonic beam. This leads to a virtual HHG source size that is significantly smaller than the NIR focus size. (c) HHG yield using Kr at a backing pressure of 4 bar as a function of the distance between the jet and the NIR focus (blue curve). The maximum XUV photon yield is observed when the jet is placed 2.5 cm behind the NIR focus. The relative NIR peak intensity as a function of the jet-focus distance (gray dotted curve) was determined using a camera, while the absolute NIR peak intensity was determined at the NIR focal plane using the measured NIR beam waist radius, pulse duration, and pulse energy. At 2.5 cm, the NIR peak intensity is 4×10^{14} W/cm^2, i.e., 25 times smaller than at the focus. Note that these are the NIR intensities at the absence of the gas jet.

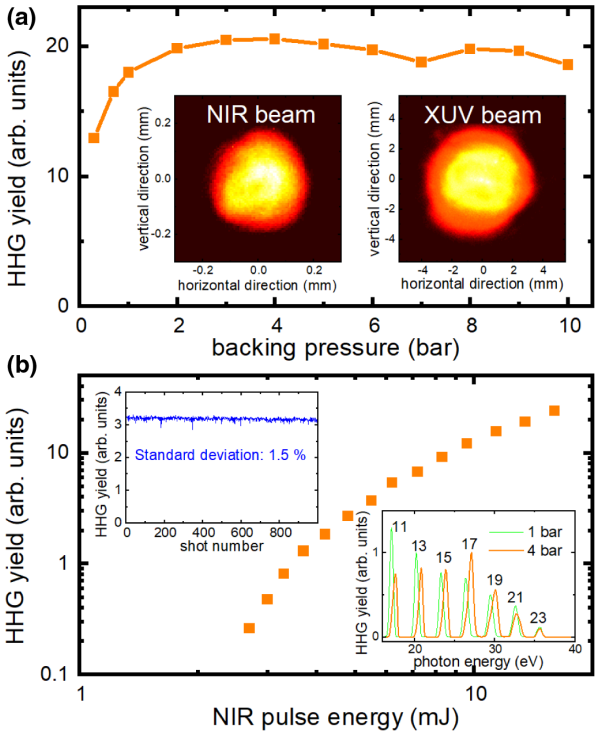

Fig. 2. Measured XUV properties. (a) HHG yield in Kr as a function of the backing pressure at a fixed jet-focus distance of 2.5 cm. The left inset shows the NIR beam profile at the position of the gas jet, and the right inset shows the XUV beam profile measured 50 cm behind the jet using a backing pressure of 4 bar. (b) Using a backing pressure of 4 bar, the HHG yield increases monotonically with the NIR pulse driving energy, as shown in a log-log plot. The very good shot-to-shot stability of the HHG yield over 1000 single shots is shown in the left inset. The right inset shows HHG spectra at backing pressures of 1 bar and 4 bar, exhibiting a clear blue shift in the latter case.

wavelengths of the generated harmonics, this curved wavefront is accompanied by a virtual HHG source size that is much smaller than the focus size of the driving laser, as we will demonstrate later. Further demagnification of the HHG source size (here, using a spherical B_4C-coated mirror with $f = 75$ mm) results in a small XUV focus size and a high XUV intensity that can be used for experiments. In the experiments to be discussed in this paper, the entire XUV beamline has a length of 2 m, which is comparable to or even smaller than most standard HHG beamlines, but a focused XUV intensity of 2×10^{14} W/cm^2 is demonstrated.

2. EXPERIMENT

To demonstrate the applicability of this scheme, we performed an experiment at the Max-Born-Institut (MBI), where high harmonics were generated in a Kr gas jet that was operated at a backing pressure of 4 bar, using 40 fs near-infrared (NIR) driving pulses with a central wavelength of 800 nm and a pulse energy of 16 mJ. Figure 1(c) shows the HHG yield as a function of the distance between the NIR focal plane and the gas jet. As a general feature, we observe two maxima of the HHG yield, one when the jet is behind the NIR focus and another one when the jet is in front of the NIR focus. For the specific parameters used in Fig. 1(c), the curve has a maximum at 2.5 cm, meaning that the jet is placed 2.5 cm—or about five Rayleigh lengths—behind the NIR focus. The NIR intensity in the absence of the gas jet at this position is 4×10^{14} W/cm^2, which is much smaller than the NIR intensity at the focus (1×10^{16} W/cm^2). Using this scheme, an XUV pulse energy of 0.3 μJ was measured using an XUV photodiode (AXUV100G), which is comparable to the results obtained with two long HHG beamlines available at the MBI [16,21].

We will show in the following that HHG far away from the NIR focus exhibits a number of favorable properties that are beneficial for applications. As depicted in Fig. 2(a), variation of the backing pressure results in an HHG yield that is almost constant for backing pressures >1 bar, making the optimization of HHG straightforward. This behavior can be explained by reshaping and phase matching, see Supplement 1 for details. The NIR beam profile measured at the jet position and the XUV beam profile measured 50 cm from the gas jet are depicted as insets in Fig. 2(a), both showing some deviations from an ideal Gaussian beam. Most importantly, our results show that the quality of the out-of-focus NIR beam profile, which is somewhat worse than the NIR beam profile at the focus, does not represent a limitation for the generation of high-flux HHG pulses. As a direct consequence of generating harmonics far away from the NIR focus, both the size and the divergence of the harmonics at the jet position are similar to the NIR beam size and divergence [cf. Fig. 1(b) and Section 3]. Correspondingly, we find that the full width at half-maximum

(FWHM) divergence of the XUV beam is similar to the NIR divergence of about 10 mrad. Figure 2(b) shows that the HHG yield increases monotonically with increasing NIR pulse energy, demonstrating that the presented HHG scheme is scalable. A further advantage is that the shot-to-shot fluctuations are low, making this a very robust source. As shown in the left inset of Fig. 2(b), a standard deviation of 1.5% was measured over 1000 single shots. Corresponding HHG spectra at backing pressures of 1 bar and 4 bar (see right inset) demonstrate that the individual harmonics are blue shifted when the pressure is increased, which provides a possibility to tune the HHG spectra. This blue shift is a consequence of propagation effects of the NIR driving laser in the gas jet [34].

3. NUMERICAL CALCULATIONS

To better understand HHG far away from the driving laser focus, we performed simulations for our experimental conditions (see Supplement 1 for a detailed list of the simulation parameters). Figure 3(a) shows how the NIR pulse is reshaped in the gas medium: The initial Gaussian spatial profile of the driving laser is modified to an almost flat-top NIR profile after propagating through the jet as a result of absorption (including losses due to ionization [35]). In this way, a stable NIR intensity of $\sim(6-9)\times 10^{13}$ W/cm^2 is achieved over a large volume. The observed regulation of the NIR peak intensity and the formation of a flat-top beam profile also explains why HHG several Rayleigh lengths away from the driving laser focus is efficient, in contrast to previous experimental observations [29]: The self-regulated beam profile makes in- and out-of-focus generation geometries similar for HHG, since efficient generation happens in the volume where the guided beam profile is formed [36]. When further increasing the distance between the NIR focus and the jet, which is accompanied by a reduction of the NIR intensity at the jet, HHG becomes less efficient because of reduced NIR reshaping effects, see also Fig. 1(c). As a consequence of reshaping, a relatively high XUV flux is observed in the simulations, which is comparable to the XUV flux that we have obtained in a simulation using an upscaled HHG source, where an NIR focal length of 9 m and an extended gas medium with a length of 20 mm were used.

The corresponding XUV beam profile at a distance of 50 cm from the gas jet presented in Fig. 3(b) exhibits a divergence similar to the experiment. This beam profile has an annular structure, which can be less or more pronounced depending on the specific parameters used in the simulations. Most importantly, the simulations show that the wavefronts of the harmonics at the detection plane are close to spherical [see Fig. 3(c) for the example of harmonic 17] and have the same radius of curvature (525 mm) as the NIR wavefronts. We note that an annular beam profile was also observed experimentally in certain conditions, but for the current experiments we chose to optimize the beam profile to be more homogeneous [see inset of Fig. 2(a)]. The difference in the XUV beam profiles might be explained by the fact that an ideal NIR Gaussian beam was used in the simulation, whereas the NIR beam used in the experiment was not an ideal Gaussian beam. As depicted in Fig. 3(d), backpropagation of the simulated XUV pulses—centered at a 55 nm wavelength—shows that the virtual HHG source is located close to the NIR focal plane and has a beam waist radius of only 3.5 μm [Fig. 3(d)], which is significantly smaller than the simulated NIR beam waist radius of 30 μm. Demagnification of the virtual XUV source using a

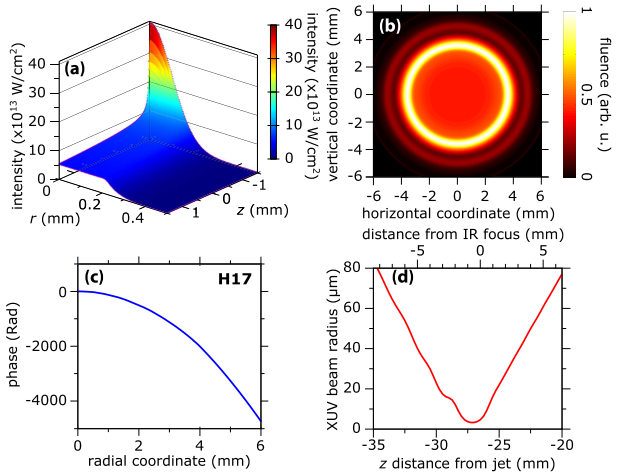

Fig. 3. Simulation of HHG far away from the NIR focus. (a) Evolution of the NIR beam profile during propagation in the Kr gas jet, with $z=0$ being the middle of the jet orifice. (b) Simulated XUV beam profile and (c) spatial phase of harmonic 17 at a distance of 50 cm from the gas jet. (d) The beam radius of the backpropagated XUV beam as a function of distance from the gas jet shows that the position of the virtual XUV source almost coincides with the NIR focal plane, which is consistent with the predictions of the modeling performed in Ref. [33].

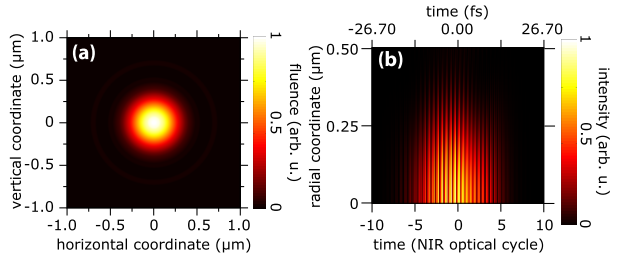

Fig. 4. Simulated spatial and temporal structure of the focused XUV field. (a) Simulated XUV beam profile at the image plane of the virtual HHG source after focusing by a 75 mm focal length spherical mirror. (b) Spatio-temporal structure of the high-harmonic field in the XUV focal plane, showing that the temporal structure is independent from the spatial coordinate, meaning that spatio-temporal couplings are minimal, consistent with predictions of Ref. [33] for HHG behind the driving laser focus.

spherical XUV focusing mirror with $f=75$ mm placed 70 cm behind the NIR focus results in an XUV beam waist radius of only 350 nm [see Fig. 4(a)], which is substantially smaller than the values achieved in loose-focusing HHG setups [14,16,17,20,26]. The spatio-temporal structure of the harmonics at the focus is presented in Fig. 4(b) and exhibits a regular shape that can be described by the multiplication of a purely spatial and a purely time dependent function, showing that spatio-temporal couplings are negligible in our scheme. Using the calculated beam waist radius in combination with the calculated XUV pulse duration of $\Delta t=25$ fs and using a pulse energy of $E=30$ nJ as available in the experiment [taking into account an aluminium (Al) filter transmission of 40% and a focusing mirror reflectivity of 25%], the theoretically achievable XUV peak intensity is estimated as $I_{\text{peak}}=2E/(\Delta t\pi w_0^2)=8\times 10^{14}\text{W/cm}^2$.

4. NONLINEAR XUV IONIZATION

The ability to generate intense XUV pulses is experimentally demonstrated by studying multiphoton absorption in Ar atoms. To this end, we generated harmonics in Xe (using a backing pressure of 2 bar and an NIR pulse energy of 8 mJ) and focused the XUV pulses into an atomic jet using a B_4C-coated spherical mirror with a focal length of 75 mm. Applying ion spatial map imaging (see Supplement 1 for details) [37,38], Ar^{2+} and Ar^{3+} ion yields were recorded along the XUV propagation direction, as shown in Figs. 5(a) and 5(b). While the Ar^+ ion yield is constant as a function of the distance from the XUV focal plane (not shown), the Ar^{2+} and Ar^{3+} ion yields are peaked at the XUV focal plane, demonstrating that these signals scale nonlinearly with the XUV intensity. The generation of Ar^{2+} from neutral Ar requires an energy of at least 43.4 eV, indicating that its generation is the result of a two-photon absorption process, considering that the maximum XUV photon energy is 27.8 eV [see Fig. 5(d)]. Indeed, the Ar^{2+} ion yield was found to scale as $I^{1.9\pm0.1}$ [see Fig. 5(e)]. Similarly, the generation of Ar^{3+} ions, which requires a minimum energy of 84.1 eV, is attributed to a four-photon absorption process. In combination with the measured XUV beam radius on the XUV focusing mirror ($w_{\mathrm{XUV,mirror}} = 7.4$ mm), the Ar^{2+} ion distribution along the XUV propagation direction [blue curve in Fig. 5(c)] can be used to estimate the Rayleigh length of the XUV beam as $z_R = 6.5$ μm (see Methods) and its waist radius as $w_0 = w_{\mathrm{XUV,mirror}}(1 + d_{\mathrm{XUV}}^2/z_R^2)^{-1/2} \approx w_{\mathrm{XUV,mirror}} z_R/d_{\mathrm{XUV}} = (600 \pm 100)$ nm, where $d_{\mathrm{XUV}} = 81$ mm is the distance between the XUV focusing mirror and the image plane. The larger value with respect to the calculated beam waist radius of 300 nm may be attributed to imperfect alignment as well as to wavefront distortions induced by the NIR pulse and the XUV focusing mirror. We further note that aberrations may affect the estimation of the XUV beam waist radius. However, since a direct measurement of the XUV beam waist radius is not possible in the normal-incidence-focusing geometry, the described method represents a good approximation. Combining this waist radius with the aforementioned XUV pulse duration of 25 fs and the pulse energy of 30 nJ, the experimental XUV peak intensity is estimated as $I_{peak} = 2 \times 10^{14}$ W/cm^2. We note that we have not observed a nonlinear XUV signal when the jet was placed at the NIR focus, although a relatively high XUV flux was observed [see Fig. 1(c)]. This underlines that the small virtual XUV source [see Fig. 3(d)] size is important for the generation of intense XUV pulses.

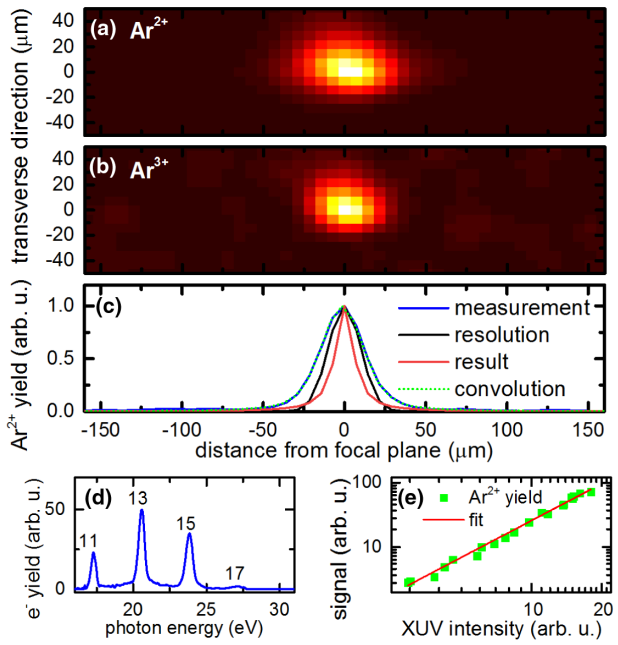

Fig. 5. XUV multiphoton ionization of Ar. (a) Ar^{2+} and (b) Ar^{3+} ion yields as a function of the distance from the XUV focal plane. The horizontal distribution is slightly narrower for Ar^{3+}, reflecting the higher nonlinearity in this case. (c) Measured Ar^{2+} ion yield (blue curve), spatial resolution (black curve), and the deconvoluted Ar^{2+} ion yield distribution (red curve). The convolution of the latter two contributions (green curve) agrees well with the measurement. (d) Photoelectron spectrum following ionization of Ar atoms by the XUV pulses, showing contributions from the harmonic orders 11 to 17. (e) Ar^{2+} ion yield as a function of the XUV intensity, which is fitted by the function $A \times I^n$, resulting in $n = 1.9 \pm 0.1$.

5. DISCUSSION AND OUTLOOK

In the future, significantly higher XUV intensities could be achieved by further scaling of our approach. We expect the XUV intensity to scale as $I_{\mathrm{XUV}} \propto E_{\mathrm{NIR}}^2$ (where E_{NIR} is the NIR pulse energy), if all relevant parameters including the NIR beam size before focusing and the XUV focusing mirror size are scaled appropriately. Using, e.g., an NIR pulse energy of 40 mJ instead of 8 mJ for HHG in Xe as well as a 5 times larger NIR beam area before focusing (using the same focusing lens), the XUV pulse energy is expected to increase by a factor of 5 due to the 5 times larger generation area, whereas the NIR focal area and the XUV virtual source area are expected to decrease by a factor of 5, resulting in a 25 times higher XUV intensity. In this case, the XUV focusing mirror needs to be able to accommodate the $\sqrt{5}$ larger XUV beam divergence. If accompanied by a reduction of the XUV pulse duration ≤ 1 fs, as has already been demonstrated for high-flux HHG sources [15,24], an intensity of 10^{17}W/cm^2 or even higher would come within reach, which, to the best of our knowledge, would significantly exceed the XUV intensities achieved at FELs and at long HHG beamlines [14,17,20,21,24] in the 15–30 eV photon energy range. This would pave the way to study dynamics that have so far only been predicted theoretically, including the control of ionization via an adiabatic passage to the continuum [39] and the study of nonperturbative strong-field effects [40]. Furthermore, sophisticated experiments such as attosecond-pump attosecond-probe spectroscopy, which require a very high degree of stability, could become significantly easier using the presented scheme.

In summary, we have demonstrated a compact setup for the generation of high XUV intensities by generating high harmonics several Rayleigh lengths away from the driving laser focus. This concept benefits from two favorable properties: (i) A large number of XUV photons are emitted from the large generation volume without the need to apply a loose-focusing geometry. (ii) XUV pulses with curved wavefronts are generated and accompanied by a small virtual XUV source size, making refocusing of the XUV pulses to a small beam waist radius possible. The small size and robustness of our concept makes it straightforward to generate intense XUV pulses in a large number of laboratories in the future. Areas that we may expect to benefit from this development are XUV-pump XUV-probe spectroscopy in gases, liquids, and solids as well as coherent diffractive imaging of nanoscale structures and nanoparticles. Furthermore, our concept is ideally suited for experiments that require either a high XUV flux or a small XUV focus.

Funding. European Regional Development Fund (GINOP-2.3.6-15-2015-00001); Institutul de Fizica Atomica (ELI_03 Pulse-MeReAd).

Acknowledgment. We thank M. Krause, R. Schumann, and C. Reiter for their support with the laser system.

Disclosures. The authors declare no conflicts of interest.

Data Availability. Data underlying the results presented in this paper are not publicly available at this time but may be obtained from the authors upon reasonable request.

Supplemental document. See Supplement 1 for supporting content.

[†]These authors contributed equally to this paper.

REFERENCES

1. P. A. Franken, A. E. Hill, C. W. Peters, and G. Weinreich, "Generation of optical harmonics," Phys. Rev. Lett. **7**, 118–119 (1961).
2. M. Bass, P. A. Franken, J. F. Ward, and G. Weinreich, "Optical rectification," Phys. Rev. Lett. **9**, 446–448 (1962).
3. M. Ferray, A. L'Huillier, X. F. Li, L. A. Lompre, G. Mainfray, and C. Manus, "Multiple-harmonic conversion of 1064 nm radiation in rare gases," J. Phys. B **21**, L31–L35 (1988).
4. R. Claps, D. Dimitropoulos, V. Raghunathan, Y. Han, and B. Jalali, "Observation of stimulated Raman amplification in silicon waveguides," Opt. Express **11**, 1731–1739 (2003).
5. D. E. Spence, P. N. Kean, and W. Sibbett, "60-fsec pulse generation from a self-mode-locked Ti:sapphire laser," Opt. Lett. **16**, 42–44 (1991).
6. R. R. Alfano and S. L. Shapiro, "Observation of self-phase modulation and small-scale filaments in crystals and glasses," Phys. Rev. Lett. **24**, 592–594 (1970).
7. T. Brabec and F. Krausz, "Intense few-cycle laser fields: frontiers of nonlinear optics," Rev. Mod. Phys. **72**, 545–591 (2000).
8. K.-L. Yeh, M. Hoffmann, J. Hebling, and K. A. Nelson, "Generation of 10 μj ultrashort terahertz pulses by optical rectification," Appl. Phys. Lett. **90**, 171121 (2007).
9. M. C. Hoffmann and J. A. Fülöp, "Intense ultrashort terahertz pulses: generation and applications," J. Phys. D **44**, 083001 (2011).
10. W. Ackermann, G. Asova, V. Ayvazyan, A. Azima, N. Baboi, J. Bähr, V. Balandin, B. Beutner, A. Brandt, A. Bolzmann, R. Brinkmann, O. I. Brovko, M. Castellano, P. Castro, L. Catani, E. Chiadroni, S. Choroba, A. Cianchi, J. T. Costello, D. Cubaynes, J. Dardis, W. Decking, H. Delsim-Hashemi, A. Delserieys, G. Di Pirro, M. Dohlus, S. Düsterer, A. Eckhardt, H. T. Edwards, B. Faatz, J. Feldhaus, K. Flöttmann, J. Frisch, L. Fröhlich, T. Garvey, U. Gensch, Ch. Gerth, M. Görler, N. Golubeva, H.-J. Grabosch, M. Grecki, O. Grimm, K. Hacker, U. Hahn, J. H. Han, K. Honkavaara, T. Hott, M. Hüning, Y. Ivanisenko, E. Jaeschke, W. Jalmuzna, T. Jezynski, R. Kammering, V. Katalev, K. Kavanagh, E. T. Kennedy, S. Khodyachykh, K. Klose, V. Kocharyan, M. Körfer, M. Kollewe, W. Koprek, S. Korepanov, D. Kostin, M. Krassilnikov, G. Kube, M. Kuhlmann, C. L. S. Lewis, L. Lilje, T. Limberg, D. Lipka, F. Löhl, H. Luna, M. Luong, M. Martins, M. Meyer, P. Michelato, V. Miltchev, W. D. Möller, L. Monaco, W. F. O. Müller, O. Napieralski, O. Napoly, P. Nicolosi, D. Nölle, T. Nuñez, A. Oppelt, C. Pagani, R. Paparella, N. Pchalek, J. Pedregosa-Gutierrez, B. Petersen, B. Petrosyan, G. Petrosyan, L. Petrosyan, J. Pflüger, E. Plönjes, L. Poletto, K. Pozniak, E. Prat, D. Proch, P. Pucyk, P. Radcliffe, H. Redlin, K. Rehlich, M. Richter, M. Roehrs, J. Roensch, R. Romaniuk, M. Ross, J. Rossbach, V. Rybnikov, M. Sachwitz, E. L. Saldin, W. Sandner, H. Schlarb, B. Schmidt, M. Schmitz, P. Schmüser, J. R. Schneider, E. A. Schneidmiller, S. Schnepp, S. Schreiber, M. Seidel, D. Sertore, A. V. Shabunov, C. Simon, S. Simrock, E. Sombrowski, A. A. Sorokin, P. Spanknebel, R. Spesyvtsev, L. Staykov, B. Steffen, F. Stephan, F. Stulle, H. Thom, K. Tiedtke, M. Tischer, S. Toleikis, R. Treusch, D. Trines, I. Tsakov, E. Vogel, T. Weiland, H. Weise, M. Wellhöfer, M. Wendt, I. Will, A. Winter, K. Wittenburg, W. Wurth, P. Yeates, M. V. Yurkov, I. Zagorodnov, and K. Zapfe, "Operation of a free-electron laser from the extreme ultraviolet to the water window," Nat. Photonics **1**, 336–342 (2007).
11. T. Shintake, H. Tanaka, T. Hara, T. Tanaka, K. Togawa, M. Yabashi, Y. Otake, Y. Asano, T. Bizen, T. Fukui, S. Goto, A. Higashiya, T. Hirono, N. Hosoda, T. Inagaki, S. Inoue, M. Ishii, Y. Kim, H. Kimura, M. Kitamura, T. Kobayashi, H. Maesaka, T. Masuda, S. Matsui, T. Matsushita, X. Maréchal, M. Nagasono, H. Ohashi, T. Ohata, T. Ohshima, K. Onoe, K. Shirasawa, T. Takagi, S. Takahashi, M. Takeuchi, K. Tamasaku, R. Tanaka, Y. Tanaka, T. Tanikawa, T. Togashi, S. Wu, A. Yamashita, K. Yanagida, C. Zhang, H. Kitamura, and T. Ishikawa, "A compact free-electron laser for generating coherent radiation in the extreme ultraviolet region," Nat. Photonics **2**, 555–559 (2008).
12. E. Allaria, R. Appio, L. Badano, W. A. Barletta, S. Bassanese, S. G. Biedron, A. Borga, E. Busetto, D. Castronovo, P. Cinquegrana, S. Cleva, D. Cocco, M. Cornacchia, P. Craievich, I. Cudin, G. D'Auria, M. Dal Forno, M. B. Danailov, R. De Monte, G. De Ninno, P. Delgiusto, A. Demidovich, S. Di Mitri, B. Diviacco, A. Fabris, R. Fabris, W. Fawley, M. Ferianis, E. Ferrari, S. Ferry, L. Froehlich, P. Furlan, G. Gaio, F. Gelmetti, L. Giannessi, M. Giannini, R. Gobessi, R. Ivanov, E. Karantzoulis, M. Lonza, A. Lutman, B. Mahieu, M. Milloch, S. V. Milton, M. Musardo, I. Nikolov, S. Noe, F. Parmigiani, G. Penco, M. Petronio, L. Pivetta, M. Predonzani, F. Rossi, L. Rumiz, A. Salom, C. Scafuri, C. Serpico, P. Sigalotti, S. Spampinati, C. Spezzani, M. Svandrlik, C. Svetina, S. Tazzari, M. Trovo, R. Umer, A. Vascotto, M. Veronese, R. Visintini, M. Zaccaria, D. Zangrando, and M. Zangrando, "Highly coherent and stable pulses from the Fermi seeded free-electron laser in the extreme ultraviolet," Nat. Photonics **6**, 699–704 (2012).
13. E. Takahashi, Y. Nabekawa, and K. Midorikawa, "Generation of 10 μj coherent extreme-ultraviolet light by use of high-order harmonics," Opt. Lett. **27**, 1920–1922 (2002).
14. A. Ravasio, D. Gauthier, F. R. N. C. Maia, M. Billon, J.-P. Caumes, D. Garzella, M. Géléoc, O. Gobert, J.-F. Hergott, A.-M. Pena, H. Perez, B. Carré, E. Bourhis, J. Gierak, A. Madouri, D. Mailly, B. Schiedt, M. Fajardo, J. Gautier, P. Zeitoun, P. H. Bucksbaum, J. Hajdu, and H. Merdji, "Single-shot diffractive imaging with a table-top femtosecond soft X-ray laser-harmonics source," Phys. Rev. Lett. **103**, 028104 (2009).
15. P. Tzallas, E. Skantzakis, L. Nikolopoulos, G. D. Tsakiris, and D. Charalambidis, "Extreme-ultraviolet pump–probe studies of one-femtosecond-scale electron dynamics," Nat. Phys. **7**, 781–784 (2011).
16. B. Schütte, M. Arbeiter, T. Fennel, M. J. Vrakking, and A. Rouzée, "Rare-gas clusters in intense extreme-ultraviolet pulses from a high-order harmonic source," Phys. Rev. Lett. **112**, 073003 (2014).
17. B. Manschwetus, L. Rading, F. Campi, S. Maclot, H. Coudert-Alteirac, J. Lahl, H. Wikmark, P. Rudawski, C. M. Heyl, B. Farkas, T. Mohamed, A. L'Huillier, and P. Johnsson, "Two-photon double ionization of neon using an intense attosecond pulse train," Phys. Rev. A **93**, 061402 (2016).
18. B. Bergues, D. E. Rivas, M. Weidman, A. A. Muschet, W. Helml, A. Guggenmos, V. Pervak, U. Kleineberg, G. Marcus, R. Kienberger, D. Charalambidis, P. Tzallas, H. Schröder, F. Krausz, and L. Veisz, "Tabletop nonlinear optics in the 100-eV spectral region," Optica **5**, 237–242 (2018).
19. A. A. Sorokin, S. V. Bobashev, T. Feigl, K. Tiedtke, H. Wabnitz, and M. Richter, "Photoelectric effect at ultrahigh intensities," Phys. Rev. Lett. **99**, 213002 (2007).
20. A. Nayak, I. Orfanos, I. Makos, M. Dumergue, S. Kühn, E. Skantzakis, B. Bodi, K. Varju, C. Kalpouzos, H. I. B. Banks, A. Emmanouilidou, D. Charalambidis, and P. Tzallas, "Multiple ionization of argon via multi-XUV-photon absorption induced by 20-GW high-order harmonic laser pulses," Phys. Rev. A **98**, 023426 (2018).
21. B. Senfftleben, M. Kretschmar, A. Hoffmann, M. Sauppe, J. Tümmler, I. Will, T. Nagy, M. J. J. Vrakking, D. Rupp, and B. Schütte, "Highly nonlinear ionization of atoms induced by intense high-harmonic pulses," J. Phys. Photon. **2**, 034001 (2020).
22. F. Bencivenga, R. Cucini, F. Capotondi, A. Battistoni, R. Mincigrucci, E. Giangrisostomi, A. Gessini, M. Manfredda, I. P. Nikolov, E. Pedersoli, E. Principi, C. Svetina, P. Parisse, F. Casolari, M. B. Danailov, M. Kiskinova, and C. Masciovecchio, "Four-wave mixing experiments with extreme ultraviolet transient gratings," Nature **520**, 205–208 (2015).
23. T. Ding, M. Rebholz, L. Aufleger, M. Hartmann, K. Meyer, V. Stooß, A. Magunia, D. Wachs, P. Birk, Y. Mi, G. D. Borisova, C. da Costa Castanheira, P. Rupprecht, Z.-H. Loh, A. R. Attar, T. Gaumnitz, S. Roling, M. Butz, H. Zacharias, S. Düsterer, R. Treusch, S. M. Cavaletto, C. Ott, and T. Pfeifer, "Nonlinear coherence effects in transient-absorption ion spectroscopy with stochastic extreme-ultraviolet free-electron laser pulses," Phys. Rev. Lett. **123**, 103001 (2019).
24. E. J. Takahashi, P. Lan, O. D. Mücke, Y. Nabekawa, and K. Midorikawa, "Attosecond nonlinear optics using gigawatt-scale isolated attosecond pulses," Nat. Commun. **4**, 2691 (2013).

25. M. J. Bogan, W. H. Benner, S. Boutet, U. Rohner, M. Frank, A. Barty, M. M. Seibert, F. Maia, S. Marchesini, S. Bajt, B. Woods, V. Riot, S. P. Hau-Riege, M. Svenda, E. Marklund, E. Spiller, J. Hajdu, and H. N. Chapman, "Single particle x-ray diffractive imaging," Nano Lett. **8**, 310–316 (2008).
26. D. Rupp, N. Monserud, B. Langbehn, M. Sauppe, J. Zimmermann, Y. Ovcharenko, T. Möller, F. Frassetto, L. Poletto, A. Trabattoni, F. Calegari, M. Nisoli, K. Sander, C. Peltz, M. J. Vrakking, T. Fennel, and A. Rouzée, "Coherent diffractive imaging of single helium nanodroplets with a high harmonic generation source," Nat. Commun. **8**, 493 (2017).
27. J.-F. Hergott, M. Kovacev, H. Merdji, C. Hubert, Y. Mairesse, E. Jean, P. Breger, P. Agostini, B. Carré, and P. Salières, "Extreme-ultraviolet high-order harmonic pulses in the microjoule range," Phys. Rev. A **66**, 021801 (2002).
28. C. M. Heyl, H. Coudert-Alteirac, M. Miranda, M. Louisy, K. Kovacs, V. Tosa, E. Balogh, K. Varjú, A. L'Huillier, A. Couairon, and C. L. Arnold, "Scale-invariant nonlinear optics in gases," Optica **3**, 75–81 (2016).
29. P. Salières, A. L'Huillier, and M. Lewenstein, "Coherence control of high-order harmonics," Phys. Rev. Lett. **74**, 3776–3779 (1995).
30. K. Kovács, B. Major, E. Balogh, C. P. Kőrös, P. Rudawski, C. M. Heyl, P. Johnsson, C. L. Arnold, A. L'Huillier, V. Tosa, and K. Varjú, "Multi-parameter optimization of a loose focusing high flux high-harmonic beamline," J. Phys. B **52**, 055402 (2019).
31. J. Li, Y. Wang, T. Guo, J. White, M. Weidman, Y. Wu, K. Hu, M. F. Jager, C. J. Kaplan, R. Geneaux, D. M. Neumark, S. R. Leone, G. G. Brown, P. Corkum, and Z. Chang, "Beam optimization in a 25 TW femtosecond laser system for high harmonic generation," J. Phys. B **53**, 145602 (2020).
32. L. Quintard, V. Strelkov, J. Vabek, O. Hort, A. Dubrouil, D. Descamps, F. Burgy, C. Péjot, E. Mével, F. Catoire, and E. Constant, "Optics-less focusing of XUV high-order harmonics," Sci. Adv. **5**, eaau7175 (2019).
33. H. Wikmark, C. Guo, J. Vogelsang, P. W. Smorenburg, H. Coudert-Alteirac, J. Lahl, J. Peschel, P. Rudawski, H. Dacasa, S. Carlström, S. Maclot, M. B. Gaarde, P. Johnsson, C. L. Arnold, and A. L'Huillier, "Spatiotemporal coupling of attosecond pulses," Proc. Natl. Acad. Sci. USA **116**, 4779–4787 (2019).
34. B. Major, M. Kretschmar, O. Ghafur, A. Hoffmann, K. Kovács, K. Varjú, B. Senfftleben, J. Tümmler, I. Will, T. Nagy, D. Rupp, M. J. J. Vrakking, V. Tosa, and B. Schütte, "Propagation-assisted generation of intense few-femtosecond high-harmonic pulses," J. Phys. Photon. **2**, 034002 (2020).
35. M. Geissler, G. Tempea, A. Scrinzi, M. Schnürer, F. Krausz, and T. Brabec, "Light propagation in field-ionizing media: extreme nonlinear optics," Phys. Rev. Lett. **83**, 2930–2933 (1999).
36. B. Major, K. Kovács, V. Tosa, P. Rudawski, A. L'Huillier, and K. Varjú, "Effect of plasma-core-induced self-guiding on phase matching of high-order harmonic generation in gases," J. Opt. Soc. Am. B **36**, 1594–1601 (2019).
37. A. T. J. B. Eppink and D. H. Parker, "Velocity map imaging of ions and electrons using electrostatic lenses: application in photoelectron and photofragment ion imaging of molecular oxygen," Rev. Sci. Instrum. **68**, 3477 (1997).
38. M. Stei, J. von Vangerow, R. Otto, A. H. Kelkar, E. Carrascosa, T. Best, and R. Wester, "High resolution spatial map imaging of a gaseous target," J. Chem. Phys. **138**, 214201 (2013).
39. U. Saalmann, S. K. Giri, and J. M. Rost, "Adiabatic passage to the continuum: controlling ionization with chirped laser pulses," Phys. Rev. Lett. **121**, 153203 (2018).
40. W.-C. Jiang, S.-G. Chen, L.-Y. Peng, and J. Burgdörfer, "Two-electron interference in strong-field ionization of He by a short intense extreme ultraviolet laser pulse," Phys. Rev. Lett. **124**, 043203 (2020).